Geochemical Perspectives Letters

Redox state of the convective mantle from CO_2-trace element systematics of oceanic basalts

J. Eguchi, R. Dasgupta

Supplementary Information

The Supplementary Information includes:

- CO_2-Nb and CO_2-Ba Mixing Calculations
- Mixing with Peridotite Melts at Different Melting Degrees
- Melting of Peridotite Enriched by Partial Melts of Recycled Lithologies
- Tables S-1 to S-4
- Figures S-1 and S-2
- Supplementary Information References

CO_2-Nb and CO_2-Ba Mixing Calculations

CO_2 concentrations used in Figure 3 were calculated using the CO_2 solubility model for natural silicate melt from Eguchi and Dasgupta (2018), which calculates dissolved CO_2 concentrations in silicate melts as a function of *P*, *T*, fO_2, and major element composition at both graphite/diamond saturated and CO_2-rich fluid saturated conditions. CO_2 concentrations were calculated at different fO_2s up to the CCO buffer, *i.e.* the highest fO_2 marking the stability of graphite/diamond, with *P-T-X* conditions in Table S-3. Nb and Ba concentrations were calculated using the batch melting equation, experimentally determined mineral modes and melt fractions, Nb and Ba partition coefficients, and lithology-specific initial Nb and Ba concentrations (Table S-1). Mixing lines between CO_2-Nb and CO_2-Ba concentrations of Siqueiros' undegassed depleted peridotite melt and graphite-saturated partial melts of subducted lithologies were generated assuming simple linear mixing. Mixing calculations for SiO_2 were calculated using wt. % SiO_2 of Siqueiros' melt inclusions (Table S-2) as the depleted endmember, and wt. % SiO_2 of experimental partial melts of recycled lithologies as the enriched endmember (Table S-3). Data used in calculations to generate Figure 3 of main text are given in Tables S-1, S-2, and S-3. We also consider the errors associated with modelled CO_2 concentrations in graphite-saturated melts. Error associated with CO_2 concentrations calculations are less than 20 % (Eguchi and Dasgupta, 2018) and do not change the interpretations made in the main text.

Mixing with Peridotite Melts at Different Melting Degrees

In order to test the sensitivity of the mixing calculations to the choice of depleted end-member, we also performed melt-melt mixing calculations by calculating CO_2 in the end-member depleted peridotite partial melt using 75 ppm CO_2 as initial concentration in the depleted mantle and $D_{CO_2}^{peridotite/basalt}$ = 0.00055 (Rosenthal *et al.*, 2015), 0.56 ppm Ba as the initial concentration of

Ba in the depleted mantle and $D_{Ba}^{peridotite/basalt}$ = 0.00012 (Workman and Hart, 2005). Figure S-1 shows how CO_2-trace element systematics of partial melt of a particular recycled lithology evolves upon mixing with peridotite partial melts of different melting degrees (F = 1-10 %). In Figure S-1, as the eclogite-derived melt end member, we use graphite-saturated eclogite partial melts generated both at high pressures (5 GPa; low-degree melt) as well as low pressures (3-2.5 GPa; higher degree melts) with fO_2s corresponding to the average fO_2 at that depth as estimated by the CLM fO_2 profile (Fig. 4). These mixing calculations confirm that high- and low-degree melts of graphite-bearing eclogite upon mixing with variable degree of oxidised peridotite partial melts also fail to reproduce the natural enriched basalts CO_2-trace element systematics.

Melting of Peridotite Enriched by Partial Melts of Recycled Lithologies

In the main text and in the supplementary discussion thus far, our mixing calculations model a scenario in which once the partial melt of a graphite-saturated subducted lithology is generated, it survives unaltered to later mix with peridotite partial melts generated at a shallower depth. This is an end-member process of contribution from recycled lithologies, which is possible if deep partial melts of subducted lithologies are transported *via* channelised flow after generation. Another end-member process of contribution from deep recycled lithologies to basalt generation, which we explore here is the complete reactive freezing of the partial melt from a graphite-saturated, silica-rich recycled lithology upon interaction with ambient peridotite, and later re-melting of this fertilised lithology at shallower, more oxidised conditions. To model this scenario, we calculate the CO_2 and Ba concentration in the graphite-saturated partial melt of a MORB-eclogite generated at 5 GPa and 1400 °C at FMQ-2.5. Then we add such partial melt of MORB-eclogite to the depleted peridotite, having a fixed CO_2 (75 ppm) and Ba (0.56 ppm, Table S-1) content. Depending on the proportion of the MORB-eclogite partial melt, the new, fertilised lithology will be variably enriched in CO_2 and Ba. We then calculate the CO_2 and Ba concentrations in partial melts of varying degrees of the new fertilised lithology which will undergo major melting at shallower, more oxidised conditions. treating CO_2 as an incompatible trace element with the CO_2 partition coefficient from Rosenthal *et al.* (2015). Treating CO_2 as an incompatible trace element in this stage requires oxidised conditions.

Figure S-2 shows the results of the two-stage melting scenario described above. Figure S-2 shows that to generate the CO_2 and Ba enrichment observed at N. Arch and the popping rocks the proportion of MORB-eclogite partial melts to get added to peridotite needs to be high (> ~10 %) and the melting degree of the fertilised lithology needs to be low (< ~0.5 %). Figure S-2 shows that very low degree melts of lithologies fertilised by high proportions of graphite-saturated partial melts of MORB-eclogite can possibly generate the high CO_2 and Ba concentrations observed in natural basalts. However, erupted basalts are likely to result from melting degrees > 0.5 %, and complete reactive crystallisation of high proportion of MORB-eclogite partial melt in a peridotite matrix is not expected. The experimental study of Mallik and Dasgupta (2012) showed that at 3 GPa for ~8 wt. % of MORB-eclogite partial melt being added to peridotite, equilibrated melt fraction is 4-5 wt. %, *i.e.* as much as half of the initial eclogite melt mass remains molten. These results demonstrate, assuming that the relationship between infiltrating melt fraction and equilibrated melt fraction as observed by Mallik and Dasgupta (2012) at 3 GPa holds across all depths of eclogite melting below the peridotite solidus, that there is a limit as to how much enrichment of CO_2 (and other trace elements) in peridotite is possible via complete reactive freezing of eclogite-derived siliceous melt. Partial reactive crystallisation of eclogite melt leads to inefficient enrichment of altered peridotite because a significant fraction of introduced CO_2 and other trace elements leaves the system in the partial melt. Therefore, the results shown in Figure S-2 for 1-5 wt. % added eclogite melt represent the maximum enrichment of the metasomatised peridotite. Therefore, we conclude that the results shown in Figure S-2 are unlikely to change the conclusions given in the main text, and even in this scenario, graphite-saturated melting of recycled lithologies cannot deliver enough CO_2 to ambient peridotite to explain natural oceanic basalts.

Supplementary Tables

Table S-1 Data used for calculation of Nb and Ba concentrations in partial melts of subducted lithologies used in Figure 3.

Lithology	P (GPa)	T (°C)	F	X_{Gt}	X_{Cpx}	refs	$D_{Nb}^{Gt/melt}$	$D_{Nb}^{Cpx/melt}$	$D_{Ba}^{Gt/melt}$	$D_{Ba}^{Cpx/melt}$	Init. Nb (ppm)	Init. Ba (ppm)	refs
Garnet-Pyroxenite	5	1650	0.19	0.53	0.28	1	0.013 (ref 5)	0.0077 (ref.4)	0.02 (ref 6)	0.02 (ref 6)	5.24	29.2	8
MORB-Eclogite	5	1400	0.21	0.33	0.46	2	0.013 (ref 5)	0.0077 (ref 4)	0.02 (ref 6)	0.02 (ref 6)	5.24	29.2	8
Metapelite	5	1400	0.41	0.41	0.59	3	0.0062 (ref 7)	0.0062 (ref 7)	0.02 (ref 6)	0.02 (ref 6)	8.94	776	9
Peridotite	-	-	0.01-0.10	-	-	-	-	-	-	-	0.15	0.56	10

Residual minerals of metapelite experiments include coesite, kyanite, and rutile in addition to garnet and clinopyroxene. Coesite, kyanite, and rutile are unlikely to hold Nb and Ba, and we are unaware of partitioning studies for these minerals, therefore we consider them to have partition coefficients of 0 when calculating the bulk partition coefficients. Bulk partition coefficients for peridotite/melt: Nb=0.0034, Ba=0.00012 from Workman and Hart (2005). Refs: [1-Kogiso *et al.* (2003), 2-Spandler *et al.*, (2008), 3-Spandler *et al.* (2010), 4-Pertermann and Hirschmann (2002), 5-Pertermann *et al.* (2004), 6-Kelemen *et al.* (2003), 7-Westrenen *et al.* (2000), 8-Gale *et al.* (2013), 9-Plank and Langmuir (1998), 10-Workman and Hart (2005)].

Table S-2 References for oceanic basalt geochemistry used in Figures 2 and 3.

Location	SiO_2 (wt. %)	CO_2 (wt. %)	Nb (ppm)	Ba (ppm)	Reference	References calling for recycled lithology in source region of basalt
Siqueiros	48.8	0.01	0.59	3	Saal *et al.* (2002)	n/a
Loihi	46.3	0.42	17	214	Dixon and Clague (2001)	Hauri (1996); Lassiter and Hauri (1998); Sobolev *et al.* (2005)
Laki	49.6	0.48	13.1	95.4	Hartley *et al.* (2014)	Shorttle *et al.* (2014); Sobolev *et al.* (2008)
Galapagos	47.4	0.58	20.84	n.m.	Koleszar *et al.* (2009)	Kurz and Geist (1999)
Pitcairn	49.6	0.79	31.1	304	Aubaud *et al.* (2006); Hekinian *et al.* (2003)	Delavault *et al.* (2016); Eisele *et al.* (2002); Woodhead and Mcculloch (1989)
N. Arch Hawaii	42.7	3.90	45	502	Dixon *et al.*, (1997); Frey *et al.* (2000)	Hauri, (1996); Lassiter and Hauri (1998); Sobolev *et al.* (2005)
Popping Rocks	49.4	5.76	29.6	194	Cartigny *et al.* (2008)	Hauri *et al.* (2017)

Unpublished Ba data for Siqueiros from Saal *et al.* (2002) is taken from Rosenthal *et al.* (2015).

Table S-3 Compilation of partial melting experiments on subducted lithologies.

P (GPa)	*T* (° C)	*F*	SiO_2	TiO_2	Al_2O_3	FeO	MnO	MgO	CaO	Na_2O	K_2O	P_2O_5	CO_2 at CCO	CO_2 at CLM fO_2
MORB-eclogite from Pertermann and Hirschmann (2003)														
3	1400	0.24	54.64	4.54	16.03	9.44	0.12	3.1	8.22	3.79	0.12	0	0.98	0.96
2	1325	0.48	52.55	2.96	17.52	9.98	0.14	4.17	8.25	4.36	0.05	0	0.93	0.87
2	1250	0.09	52.42	6.66	14.49	11.41	0.12	3.25	7.74	3.74	0.16	0	0.95	0.88
2.5	1325	0.2	58.42	4.23	15.51	8.25	0.1	2.53	7.06	3.78	0.13	0	0.83	0.82
3	1315	0.02	55.19	6.07	14.71	9.06	0.1	2.22	7.84	3.68	1.14	0	1.24	1.23
3	1325	0.05	56.35	6.25	14.94	8.42	0.09	2.31	6.92	4.2	0.51	0	1.05	1.04
3	1335	0.03	55.98	6.65	14.92	8.37	0.09	2.13	7.28	4.02	0.57	0	1.05	1.04
3	1335	0.07	57.22	5.66	15.35	8.02	0.1	2.28	7.14	3.94	0.28	0	0.99	0.99
3	1335	0.03	57.33	6.18	14.93	7.54	0.09	2.24	7.12	4.09	0.49	0	1.02	1.02
3	1335	0.02	56.62	6.47	14.93	7.91	0.09	2.19	6.83	4.14	0.81	0	1.02	1.02
3	1350	0.08	56.03	6.38	15.31	8.27	0.09	2.39	7.44	3.77	0.31	0	0.98	0.97
3	1365	0.09	56.07	5.89	15.37	8.34	0.1	2.44	7.61	3.95	0.24	0	0.98	0.96
3	1375	0.18	57.00	4.64	15.69	8.46	0.09	2.75	7.42	3.82	0.13	0	0.90	0.90
3	1425	0.36	53.47	3.77	15.79	9.87	0.17	4	8.98	3.35	0.07	0	1.05	1.02
3	1450	0.51	51.89	3.19	16.49	10.15	0.15	4.61	9.42	3.5	0.07	0	1.13	1.09
2	1325	0.52	52.81	2.74	17.1	9.36	0.13	4.02	8.05	4.21	0.52	0	0.93	0.87
3	1275	0.14	63.64	3.33	15.35	5.18	0.06	1.53	4.93	4.34	1.63	0	1.15	1.16
3	1315	0.15	61.49	4.12	14.52	6.2	0.06	1.98	6.16	4.01	1.44	0	1.03	1.04
Bi-mineralic eclogite from Kogiso and Hirschmann (2006)														
3	1470	0.28	46.4	3.9	13.4	13.2	0.19	7.3	11.6	3.7	0.03	0	2.41	2.26
5	1600	0.6	47.4	2.2	10.9	13.9	0.17	9.4	12.3	2.8	0.04	0	1.83	0.47
5	1600	0.38	45.7	3.6	12.8	14	0.24	7.4	12.6	3	0.06	0	1.65	0.43
MORB-eclogite from Spandler *et al.* (2008)														
4	1450	0.53	53.69	2.9	15.67	9.79	0	4.77	8.41	3.65	0.77	0.25	1.12	0.64
3	1240	0.04	63.6	2.56	15.69	3.64	0	1.22	3.45	4.31	4.36	1.18	1.43	1.44
3	1260	0.1	63.23	2.99	15.41	4.28	0	1.42	3.47	5.03	3.27	0.89	1.27	1.29
3	1280	0.21	63.99	2.77	15.25	4.66	0	1.67	4.34	5.21	1.75	0.37	1.16	1.17
3	1320	0.24	61.57	2.83	15.68	5.96	0	1.96	5.09	4.91	1.62	0.39	1.02	1.03
3	1360	0.36	57.86	2.94	16.32	7.54	0	3.02	6.54	4.53	1.05	0.19	0.99	0.98
3	1400	0.61	53.64	2.25	16.72	9.08	0	5.38	8.32	4.02	0.58	0	1.20	1.17
3	1440	0.85	52.00	2	16.42	9.1	0	7.04	9.19	3.5	0.46	0.21	1.32	1.27
4	1280	0.07	66.08	2.67	13.92	4.13	0	1.02	2.75	3.2	5.59	0.66	1.49	0.57
4	1320	0.1	62.68	3.72	14.45	5.07	0	1.32	3.61	3.35	4.83	0.97	1.23	0.52
4	1360	0.19	60.34	4.09	14.18	6.83	0	2.36	5.98	3.76	1.96	0.5	1.08	0.49
4	1400	0.23	58.4	4.13	14.3	7.81	0	2.9	6.53	3.7	1.65	0.59	0.99	0.50
4	1500	0.86	51.66	1.95	16.02	9.69	0	7.15	9.38	3.53	0.46	0.16	1.27	0.81
5	1300	0.04	65.15	3.51	13.63	3	0	0.97	2.51	2.44	7.72	1.06	1.57	0.18
5	1350	0.07	60.58	5.66	12.83	5.43	0	1.69	4.24	2.67	5.58	1.02	1.17	0.14
5	**1400**	**0.21**	**58.12**	**4.37**	**13.82**	**8.16**	**0**	**2.89**	**6.92**	**3.44**	**1.74**	**0.53**	**1.02**	**0.14**
5	1500	0.46	53.93	3.17	15.14	9.9	0	4.65	8.39	3.59	0.89	0.33	0.90	0.17
5	1550	0.68	54.42	2.35	15.76	9.62	0	6.35	9.17	3.52	0.58	0.23	0.87	0.19

Table S-3 Continued

MORB-eclogite from Yaxley and Green (1998)														
3.5	1250	0.13	64.70	2.70	14.70	4.20	0.00	1.40	3.90	4.10	3.60	0.80	1.51	1.05
3.5	1300	0.13	63.20	3.00	14.70	4.90	0.10	1.00	4.00	4.30	3.80	0.90	1.28	1.02
3.5	1350	0.33	57.90	2.80	15.10	8.40	0.10	2.20	7.50	4.50	1.10	0.40	1.30	1.16
3.5	1450	0.71	51.60	1.90	16.20	10.30	0.10	6.00	9.20	3.70	0.60	0.30	1.38	1.38
3.5	1475	0.86	51.60	1.50	16.20	9.80	0.20	6.90	9.80	3.20	0.50	0.30	1.36	1.38
Pyroxenite from Kogiso *et al.* (2003)														
5	**1650**	**0.19**	**46.75**	**3.13**	**6.38**	**13.86**	**0.14**	**13.39**	**13.6**	**2.25**	**0.05**	**0**	**2.70**	**0.81**
Pyroxenite from Keshav *et al.* (2004)														
2.5	1400	0.42	44.14	1.19	13.61	13.01	0.19	13.69	9.94	2.58	1.01	0	2.83	2.58
2	1360	0.35	44.43	1.43	13.97	12.83	0.19	13.39	9.91	2.17	0.89	0	2.20	1.97
2	1340	0.21	44.12	1.51	13.18	13.37	0.19	12.94	9.69	2.58	1.02	0	2.50	2.18
2.5	1370	0.18	43.82	1.37	12.94	13.91	0.19	12.87	9.85	2.89	1.27	0	3.22	2.92
Pyroxenite from Lambart *et al.* (2009)														
1	1230	0.05	52.57	0.21	19.71	5.48	0.07	7.92	8.9	4.7	0.37	0	0.54	0.50
1	1250	0.12	51.62	0.17	17.99	6.43	0.11	9.79	10.42	3.16	0.16	0	0.65	0.59
1.5	1280	0.03	48.8	0.36	18.31	7.12	0.11	10.79	10.06	3.83	0.48	0	1.30	1.20
1.5	1290	0.04	49.77	0.33	17.21	7.23	0.11	11.34	10.21	3.37	0.38	0	1.28	1.16
1.5	1290	0.02	51	0.31	17.45	6.91	0.12	10.3	9.62	3.83	0.47	0	1.13	1.06
1	1200	0.04	48.03	1.65	16.6	13.2	0.25	7.18	8.28	4.49	0.4	0	0.67	0.56
1	1225	0.11	48.8	1.64	17.8	11	0.32	7.36	9.2	3.56	0.25	0	0.60	0.51
1	1240	0.39	49.36	0.8	18.87	9.4	0.13	7.98	9.99	3.23	0.21	0	0.61	0.53
1.5	1200	0.03	52.66	1.09	20.19	7.51	0.13	4.29	5.73	6.74	1.63	0	0.81	0.77
1.5	1230	0.03	52.63	1.06	19.79	8.15	0.14	4.68	5.78	6.43	1.32	0	0.75	0.70
1.5	1250	0.14	50.62	1.08	19.67	10.01	0.15	5.78	6.74	5.4	0.53	0	0.75	0.68
1	1185	0.14	44.71	1.46	15.78	19.85	0.33	5.45	9.71	2.52	0.17	0	0.69	0.60
1	1225	0.42	44.04	1.33	15.32	18.4	0.37	7.43	11.58	1.46	0.08	0	0.96	0.89
1	1250	0.53	43.58	1.05	15.24	17.34	0.36	8.29	12.74	1.31	0.06	0	1.19	1.09
1.5	1230	0.03	42.43	2.28	13.68	23.23	0.37	5.55	8.49	2.83	1.13	0	1.64	1.52
1.5	1250	0.09	41.55	1.59	14.63	21.78	0.36	7.48	9.81	2.46	0.32	0	1.70	1.52
1.5	1270	0.32	43	1.19	13.68	21.21	0.37	8.4	10.7	1.29	0.09	0	1.77	1.70
1.5	1290	0.43	42.86	1.18	13.67	19.94	0.36	9.13	11.58	1.22	0.05	0	2.00	1.90
Pyroxenite from Lambart *et al.* (2012)														
2.5	1400	0.045	48.7	1.9	14.6	12.2	0.19	8.4	8.4	4.15	1.42	0	1.82	1.66
2.5	1400	0.22	39.1	2.36	10.4	22.2	0.37	10.6	12.8	1.94	0.18	0	5.45	5.11
Eclogite Residual from Rosenthal *et al.* (2014)														
4	1400	0.05	57.1	4.5	12.4	7.06	0	1.29	7.41	2.53	0	0	0.89	0.45
3	1250	0.01	65.11	1.9	16.16	4.29	0	1.07	3.71	4.08	0	0	0.99	1.01
3	1250	0.01	62.22	2.54	15.53	5.28	0	1.58	5.25	3.05	0	0	1.02	1.02
3	1225	0.05	67.37	1.67	16.48	4.18	0	1.27	3.98	3.58	0	0	1.14	1.16
3	1275	0.05	63.79	2.28	15.75	4.75	0	1.23	4.68	2.99	0	0	0.94	0.96
3	1300	0.16	60	2.42	16.48	7.18	0	1.74	6.18	3.6	0	0	1.00	1.00
3	1350	0.24	56.11	2.15	16.29	8.11	0	2.06	6.75	3.71	0	0	0.91	0.91
3	1400	0.31	55.19	1.58	18.61	9.73	0	2.23	6.46	4.34	0	0	0.80	0.80
3	1450	0.95	49.18	1.13	17.46	10.37	0	9.11	9.77	2.81	0	0	1.42	1.37
3	1475	1	50.01	1.1	18.13	5.9	0	9.76	9.64	2.73	0	0	1.21	1.19

Table S-3 continued

4	1450	0.13	57.81	2.87	13.04	5.82	0	2.02	9.21	2.87	0	0	0.98	0.55
Secondary Pyroxenite from Sobolev *et al.* (2007)														
3.5	1400	0.08	60.7	2.76	14.4	6.8	0.068	4.44	7.71	2.34	0.7	0	0.88	0.88
3.5	1450	0.16	55.76	2.33	14.2	7.63	0.081	7.45	7.95	2.16	0.44	0	0.93	0.94
3.5	1500	0.33	53.3	1.58	14.21	8.25	0.106	10.67	8.61	1.75	0.13	0	1.07	1.06
3.5	1520	0.42	52.54	1.29	14.22	8.65	0.112	11.66	8.65	1.98	0.14	0	1.14	1.12
Basalt+Peridotite from Kogiso *et al.* (1998)														
1.5	1300	0.14	49.09	2.18	19.3	8.24	0	7.29	5.95	7.04	0.88	0	0.87	0.79
2	1350	0.08	47.38	2.5	17.92	10.23	0	8.48	5.63	6.25	1.57	0	1.24	1.12
1.5	1300	0.09	50.55	1.96	19.86	6.37	0	7.12	5.79	7.29	1.04	0	0.82	0.77
2	1350	0.04	49.03	1.82	19.08	8.05	0	7.99	5.51	5.91	2.56	0	1.12	1.04
Metapelite from Spandler *et al.* (2010)														
3	1200	0.04	67.29	1.44	16.63	1.9	0	0.6	2.01	3.96	5.43	0.73	1.62	1.61
3	1230	0.28	67.15	1.48	16.44	2.18	0	0.73	2.2	3.98	5.18	0.66	1.60	1.58
3	1260	0.62	66.94	0.85	16.86	2.62	0	0.91	2.55	4.06	4.91	0.3	1.46	1.45
3	1300	0.69	66.2	0.86	16.89	3.42	0	1.28	2.86	3.69	4.47	0.33	1.20	1.19
3	1350	0.77	65.62	0.79	16.84	4.43	0	1.82	2.89	3.34	3.93	0.34	0.96	0.94
3	1400	0.89	65.45	0.71	16.54	5.16	0	2.81	2.77	2.92	3.33	0.32	0.74	0.75
4	1250	0.22	67.66	1.26	15.91	2.09	0	0.5	1.12	2.72	7.97	0.77	1.90	0.73
4	1300	0.44	67.18	0.97	15.91	2.61	0	0.71	1.64	3.85	6.69	0.44	1.62	0.67
5	**1400**	**0.41**	**65.24**	**1.08**	**15.85**	**3.65**	**0**	**1.1**	**2.17**	**3.48**	**6.98**	**0.45**	**1.05**	**0.16**
5	1450	0.69	65.06	0.92	16.44	4.32	0	1.8	3.01	3.78	4.31	0.37	0.80	0.14
5	1500	0.87	65.11	0.72	16.65	5.06	0	2.8	2.82	3.06	3.51	0.27	0.59	0.12
5	1600	0.97	68.04	0.68	15.3	4.86	0	2.53	2.53	2.61	3.19	0.27	0.43	0.13

All values for oxides have units of wt. %. Experimental partial melts reported in bold text are experiments used to generate Figure 3 of main text. References used for solidi in Figure 1: Metapelite - Spandler *et al.* (2010), MORB-eclogite Spandler *et al.* (2008), Garnet-pyroxenite Kogiso *et al.* (2003), peridotite-Hirschmann (2000). CO_2 at CCO and CO_2 at CLM fO_2 refer to the calculated CO_2 contents (in wt. %) at graphite saturation for the respective partial melts at the *P-T* conditions of their generation based on the model of Eguchi and Dasgupta (2018).

Table S-4 Xenolith data used in Figure 4.

Xenolith type	P (GPa)	log fO_2 (ΔFMQ)	Location	n	Reference
Peridotite	2.1 to 7.1	-5.1 to 1.5	Kaapvaal, Slave, Siberian cratons	163	(Stagno *et al.*, 2015)
Eclogite	3.1 to 5.4	-3.1 to -0.1	Lahotojoki, Udachnaya, Robert Victor, Dabie-sulu	12	(Stagno *et al.*, 2015)
Peridotite	2.0 to 7.4	-3.9 to 0.2	Slave craton	45	(Yaxley *et al.*, 2017)
Eclogite	4.7 to 6.5	-4.6 to -1.3	Kaapvaal craton	15	(Aulbach *et al.*, 2017)
Eclogite	4.4 to 6.8	-4.6 to -0.5	Slave craton	24	(Smart *et al.*, 2017)

fO_2 values were not recalculated here. fO_2 values reported in references are used for Figure 4.

Supplementary Figures

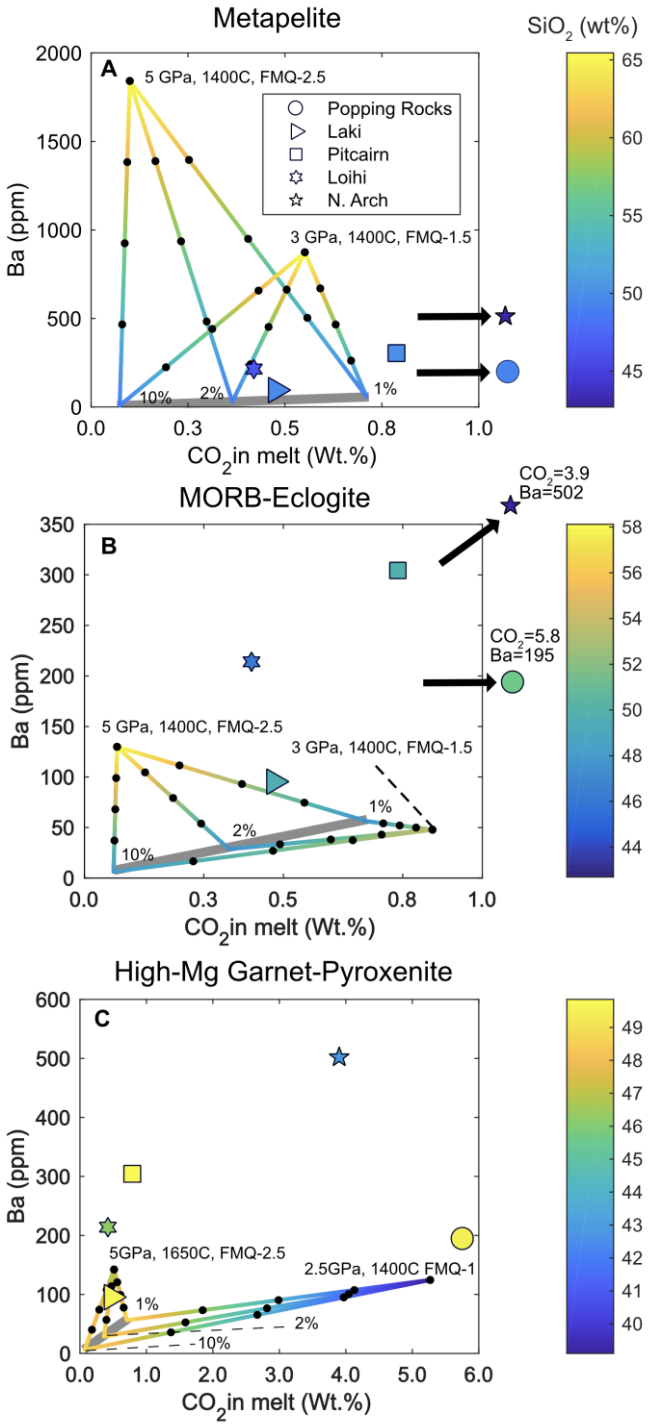

Figure S-1 CO_2-Ba mixing lines between graphite-saturated partial melts of subducted lithologies and different degrees of partial melts (*F*=1-10%, gray band) of peridotite compared with CO_2-Ba data of minimally degassed oceanic basalts. Text in figures shows the *P-T-fO*$_2$ conditions used to calculate CO_2 concentrations in the graphite-saturated partial melt of the subducted lithologies, where *P-fO*$_2$ roughly corresponds to depth-*fO*$_2$ profile estimated from continental lithospheric mantle samples (Fig. 4). Percentages correspond to melting degrees used to calculate CO_2 and Ba in the partial melt of peridotite. Black circles along mixing lines denote 25 wt. % incremental addition of partial melts from various recycled lithologies. SiO_2 content of peridotite partial melts are calculated at 2.5 GPa as a function of *F* using the parametrisation provided by Ding and Dasgupta (2018).

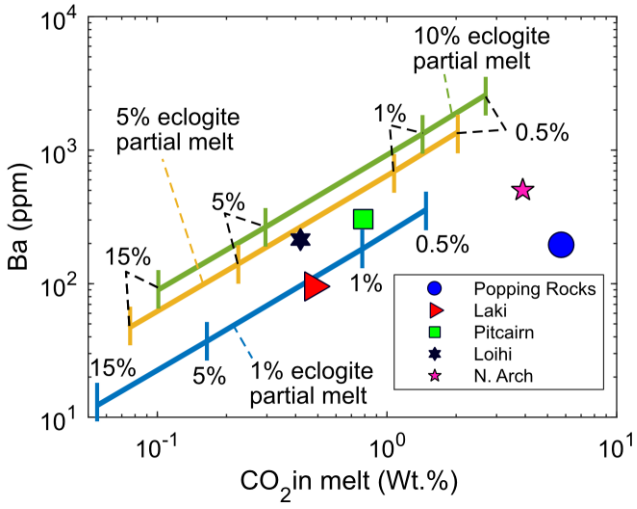

Figure S-2 CO_2-Ba systematics of calculated model peridotite partial melts compared with highest CO_2-Ba data of oceanic basalts from literature. The extent of peridotite melting varying between 0.5 and 15 % where the peridotite has undergone a prior stage of enrichment *via* reactive freezing of partial melts derived from graphite-saturated MORB-eclogite at depths. Initial CO_2-Ba concentrations of the fertilised peridotitic lithology are calculated *via* linear mixing of CO_2-Ba concentrations of depleted peridotite (75 ppm CO_2; 0.56 ppm Ba) and graphite-saturated partial melts of MORB-eclogite. Contributions by wt. % of MORB-eclogite melt are labeled on the figure (1 %, 5 %, and 10 %). Ticks along individual melting lines denote the degree of melting of the enriched, fertilised lithology (0.5, 1, 5, 15). CO_2 and Ba concentrations of partial melts are calculated assuming both C and Ba behave as highly incompatible elements (*i.e.*, partition coefficient of carbon from Rosenthal *et al*., 2015) during shallow melting of peridotite, *i.e.*, under relatively oxidising conditions, where no carbon-rich phase remains in the peridotite residue. The figure shows that a two-stage melting model (with graphite-saturated eclogite melting being the first stage) cannot explain the combined CO_2-Ba systematics of N. Arch and Popping Rocks, given complete reactive freezing of MORB-eclogite partial melt in a peridotite matrix is possible only at very low melt:rock ratio (~1 wt. %; Mallik and Dasgupta, 2012)

Supplementary Information References

Aubaud, C., Pineau, F., Hékinian, R., Javoy, M. (2006) Carbon and hydrogen isotope constraints on degassing of CO_2 and H_2O in submarine lavas from the Pitcairn hotspot (South Pacific). *Geophysical Research Letters* 33, L02308.

Aulbach, S., Woodland, A.B., Vasilyev, P., Galvez, M.E., Viljoen, K.S. (2017) Effects of low-pressure igneous processes and subduction on Fe $^{3+}/\Sigma$Fe and redox state of mantle eclogites from Lace (Kaapvaal craton). *Earth and Planetary Science Letters* 474, 283–295.

Cartigny, P., Pineau, F., Aubaud, C., Javoy, M. (2008) Towards a consistent mantle carbon flux estimate: Insights from volatile systematics (H_2O/Ce, δD, CO_2/Nb) in the North Atlantic mantle (14° N and 34° N). *Earth and Planetary Science Letters* 265, 672–685.

Delavault, H., Chauvel, C., Thomassot, E., Devey, C.W., Dazas, B. (2016) Sulfur and lead isotopic evidence of relic Archean sediments in the Pitcairn mantle plume. *Proceedings of the National Academy of Sciences*. National Academy of Sciences 113, 12952–12956.

Ding, S., Dasgupta, R. (2018) Sulfur inventory of ocean island basalt source regions constrained by modeling the fate of sulfide during decompression melting of a heterogeneous mantle. *Journal of Petrology*, egy061, doi: 10.1093/petrology/egy061.

Dixon, J.E., Clague, D.A. (2001) Volatiles in Basaltic Glasses from Loihi Seamount, Hawaii: Evidence for a Relatively Dry Plume Component. *Journal of Petrology* 42, 627–654.

Dixon, J.E., Clague, D.A., Wallace, P., Poreda, R. (1997) Volatiles in Alkalic Basalts from the North Arch Volcanic Field, Hawaii: Extensive Degassing of Deep Submarine-erupted Alkalic Series Lavas. *Journal of Petrology* 38, 911–939.

Eguchi, J., Dasgupta, R. (2018) A CO_2 solubility model for silicate melts from fluid saturation to graphite or diamond saturation. *Chemical Geology* 487, 23–38.

Eisele, J., Sharma, M., Galer, S.J.G., Blichert-Toft, J., Devey, C.W., Hofmann, A.W. (2002) The role of sediment recycling in EM-1 inferred from Os, Pb, Hf, Nd, Sr isotope and trace element systematics of the Pitcairn hotspot. *Earth and Planetary Science Letters* 196, 197–212.

Frey, F.A., Clague, D.A., Mahoney, J.J., Sinton, J.M. (2000) Volcanism at the Edge of the Hawaiian Plume: Petrogenesis of Submarine Alkalic Lavas from the North Arch Volcanic Field. *Journal of Petrology* 41, 667–691.

Gale, A., Dalton, C.A., Langmuir, C.H., Su, Y., Schilling, J.-G. (2013) The mean composition of ocean ridge basalts. *Geochemistry, Geophysics, Geosystems* 14, 489–518.

Hartley, M.E., Maclennan, J., Edmonds, M., Thordarson, T. (2014) Reconstructing the deep CO_2 degassing behaviour of large basaltic fissure eruptions. *Earth and Planetary Science Letters* 393, 120–131.

Hauri, E.H. (1996) Major-element variability in the Hawaiian mantle plume. *Nature* 382, 415–419.

Hauri, E.H., Maclennan, J., McKenzie, D., Gronvold, K., Oskarsson, N., Shimizu, N. (2017) CO_2 content beneath northern Iceland and the variability of mantle carbon. *Geology* 46, 55–58.

Hekinian, R. *et al.* (2003) The Pitcairn hotspot in the South Pacific: distribution and composition of submarine volcanic sequences. *Journal of Volcanology and Geothermal Research* 121, 219–245.

Hirschmann, M.M. (2000) Mantle solidus: Experimental constraints and the effects of peridotite composition. *Geochemistry, Geophysics, Geosystems* 1.

Kelemen, P.B., Yogodzinski, G.M., Scholl, D.W. (2003) Along-strike variation in the Aleutian Island Arc: Genesis of high Mg# andesite and implications for continental crust. In: Eiler, J. (Ed.) *Inside the Subduction Factory. Volume 138, Geophysical Monograph Series.* American Geophysical Union, Washington D.C., 223–276.

Keshav, S., Gudfinnsson, G.H., Sen, G., Fei, Y. (2004) High-pressure melting experiments on garnet clinopyroxenite and the alkalic to tholeiitic transition in ocean-island basalts. *Earth and Planetary Science Letters* 223, 365–379.

Kogiso, T., Hirschmann, M.M. (2006) Partial melting experiments of bimineralic eclogite and the role of recycled mafic oceanic crust in the genesis of ocean island basalts. *Earth and Planetary Science Letters* 249, 188–199.

Kogiso, T., Hirose, K., Takahashi, E. (1998) Melting experiments on homogeneous mixtures of peridotite and basalt: application to the genesis of ocean island basalts. *Earth and Planetary Science Letters* 162, 45–61.

Kogiso, T., Hirschmann, M.M., Frost, D.J. (2003) High-pressure partial melting of garnet pyroxenite: Possible mafic lithologies in the source of ocean island basalts. *Earth and Planetary Science Letters* 216, 603–617.

Koleszar, A.M., Saal, A.E., Hauri, E.H., Nagle, A.N., Liang, Y., Kurz, M.D. (2009) The volatile contents of the Galapagos plume; evidence for H2O and F open system behavior in melt inclusions. *Earth and Planetary Science Letters* 287, 442–452.

Kurz, M.D., Geist, D. (1999) Dynamics of the Galapagos hotspot from helium isotope geochemistry. *Geochimica et Cosmochimica Acta* 63, 4139–4156.

Lambart, S., Laporte, D., Schiano, P. (2009) An experimental study of pyroxenite partial melts at 1 and 1.5 GPa: Implications for the major-element composition of Mid-Ocean Ridge Basalts. *Earth and Planetary Science Letters* 288, 335–347.

Lambart, S., Laporte, D., Provost, A., Schiano, P. (2012) Fate of pyroxenite-derived melts in the peridotitic mantle: Thermodynamic and experimental constraints. *Journal of Petrology* 53, 451–476.

Lassiter, J.C., Hauri, E.H. (1998) Osmium-isotope variations in Hawaiian lavas: evidence for recycled oceanic lithosphere in the Hawaiian plume. *Earth and Planetary Science Letters* 164, 483–496.

Mallik, A., Dasgupta, R. (2012) Reaction between MORB-eclogite derived melts and fertile peridotite and generation of ocean island basalts. *Earth and Planetary Science Letters* 329–330, 97–108.

Pertermann, M., Hirschmann, M.M. (2002) Trace-element partitioning between vacancy-rich eclogitic clinopyroxene and silicate melt. *American Mineralogist* 87, 1365–1376.

Pertermann, M., Hirschmann, M.M. (2003) Anhydrous Partial Melting Experiments on MORB-like Eclogite: Phase Relations, Phase Compositions and Mineral-Melt Partitioning of Major Elements at 2-3 GPa. *Journal of Petrology* 44, 2173–2201.

Pertermann, M., Hirschmann, M.M., Hametner, K., Günther, D., Schmidt, M.W. (2004) Experimental determination of trace element partitioning between garnet and silica-rich liquid during anhydrous partial melting of MORB-like eclogite. *Geochemistry, Geophysics, Geosystems* 5.

Plank, T., Langmuir, C.H. (1998) The chemical composition of subducting sediment and its consequences for the crust and mantle. *Chemical Geology* 145, 325–394.

Rosenthal, A., Yaxley, G.M., Green, D.H., Hermann, J., Kovács, I., Spandler, C. (2014) Continuous eclogite melting and variable refertilisation in upwelling heterogeneous mantle. *Scientific reports* 4, 6099.

Rosenthal, A., Hauri, E.H., Hirschmann, M.M. (2015) Experimental determination of C, F, and H partitioning between mantle minerals and carbonated basalt, CO2/Ba and CO2/Nb systematics of partial melting, and the CO2 contents of basaltic source regions. *Earth and Planetary Science Letters* 412, 77–87.

Saal, A.E., Hauri, E.H., Langmuir, C.H., Perfit, M.R. (2002) Vapour undersaturation in primitive mid-ocean-ridge basalt and the volatile content of Earth's upper mantle. *Nature* 419, 451–455.

Shorttle, O., Maclennan, J., Lambart, S. (2014) Quantifying lithological variability in the mantle. *Earth and Planetary Science Letters* 395, 24–40.

Smart, K.A., Tappe, S., Simonetti, A., Simonetti, S.S., Woodland, A.B., Harris, C. (2017) Tectonic significance and redox state of Paleoproterozoic eclogite and pyroxenite components in the Slave cratonic mantle lithosphere, Voyageur kimberlite, Arctic Canada. *Chemical Geology* 455, 98–119.

Sobolev, A.V, Hofmann, A.W., Sobolev, S.V, Nikogosian, I.K. (2005) An olivine-free mantle source of Hawaiian shield basalts. *Nature* 434, 590–597.

Sobolev, A.V. *et al.* (2007) The Amount of Recycled Crust in Sources of Mantle - Derived Melts. *Science* 316, 412–417.

Sobolev, A.V, Hofmann, A.W., Brügmann, G., Batanova, V.G., Kuzmin, D.V. (2008) A Quantitative Link Between Recycling and Osmium Isotopes. *Science* 321, 536–536.

Spandler, C., Yaxley, G., Green, D.H., Rosenthal, A. (2008) Phase Relations and Melting of Anhydrous K-bearing Eclogite from 1200 to 1600 C and 3 to 5 GPa. *Journal of Petrology* 49, 771–795.

Spandler, C., Yaxley, G., Green, D.H., Scott, D. (2010) Experimental phase and melting relations of metapelite in the upper mantle: Implications for the petrogenesis of intraplate magmas. *Contributions to Mineralogy and Petrology* 160, 569–589.

Stagno, V., Frost, D.J., McCammon, C.A., Mohseni, H., Fei, Y. (2015) The oxygen fugacity at which graphite or diamond forms from carbonate-bearing melts in eclogitic rocks. *Contributions to Mineralogy and Petrology* 169, 16.

van Westrenen, W., Blundy, J.D., Wood, B.J. (2000) Effect of Fe^{2+} on garnet–melt trace element partitioning: experiments in FCMAS and quantification of crystal-chemical controls in natural systems. *Lithos* 53, 189–201.

Woodhead, J.D., Mcculloch, M.T. (1989) Ancient seafloor signals in Pitcairn Island lavas and evidence for large amplitude, small length-scale mantle heterogeneities. *Earth and Planetary Science Letters* 94, 257–213.

Workman, R.K., Hart, S.R. (2005) Major and trace element composition of the depleted MORB mantle (DMM). *Earth and Planetary Science Letters* 231, 53–72.

Yaxley, G.M., Green, D.H. (1998) Reactions between eclogite and peridotite: Mantle refertilisation by subduction of oceanic crust. *Schweizerische Mineralogische Und Petrographische Mitteilungen* 78, 243–255.

Yaxley, G.M., Berry, A.J., Rosenthal, A., Woodland, A.B., Paterson, D. (2017) Redox preconditioning deep cratonic lithosphere for kimberlite genesis - Evidence from the central Slave Craton. *Scientific Reports* 7, doi: 10.1038/s41598-017-00049-3.